30th Annual International IEEE EMBS Conference
Vancouver, British Columbia, Canada, August 20-24, 2008

Robust Optic Disc Location via Combination of Weak Detectors

Adria Perez-Rovira and Emanuele Trucco

Abstract— **This paper presents a new robust approach for the automatic location of the optic disc. We detect several candidates independently for optic disc, macula and the main blood vessels (arcades). Candidates are sorted by reliability. The space of all possible triplets disc-macula-arcades is searched using a-priori anatomical knowledge, selecting the triplet formed by the most reliable candidates satisfying anatomical constraints best. This triplet includes the best optic disc location. The approach was tested using the well-known STARE data set (81 images: 31 healthy retinas and 50 containing pathological lesions of various types and severity) and 20 wide-field-of-view scanning laser ophthalmoscope (SLO) images acquired with an OPTOS instrument. We achieved 91.4% detection rate in the STARE data set and 100% in the OPTOS data set.**

I. Introduction

We present a new robust approach for the automatic location of the optic disc (henceforth OD) combining weak detectors of retinal landmarks and anatomical knowledge.

Several algorithms have been presented to detect the OD in fundus images of the retina. Some approaches have been based on context; for instance, Hoover and Goldbaum [6] use the fuzzy convergence of the blood vessels to locate the OD; Foracchia et al. [4] fit a geometric model of vessel structure over a network of detected vessels; Niemeijer et al. [7] use a combination of local and global cues. Other authors have taken shape-based approaches; e.g., Fleming et al. [2] deploy a Generalized Hough transform to detect the circular shape of the OD; Osareh et al. [8] use an automatically initialized snake to detect the OD boundary. Others have considered properties if the intensity pattern of the OD; e.g., Sinthanayothin et al. [9] identify the OD as the region of maximum intensity variance.

In this paper, we take forward the idea presented in [10], i.e., constraint satisfaction to combine different landmarks in the retina, but with more efficient, independent detectors and a new rating (reliability) system for the positions of the OD and macula given the arcades, removing the threshold used previously. These new features increase the quality of the results.

The remainder of this paper is organized as follows. The method is described in Section 2; in Section 3 experimental results are presented, using two data sets: the well-known STARE collection, used by several authors, and wide-field-of-view SLO images acquired with an OPTOS instrument. Finally, in Section 4 the results are discussed and compared with other methods to locate the OD.

This work was supported by a Northern Research Partnership studentship and OPTOS plc.

The authors are with the School of Computing, University of Dundee, Dundee, DD1 4HN, UK e.trucco@dundee.ac.uk, arovirez@computing.dundee.ac.uk

II. Method

The idea behind this work is to generate several location hypotheses for the main retinal landmarks (OD, macula and arcades) using independent weak detectors, to leverage contextual evidence about the location of the OD. Each landmark candidate is rated for its reliability, and a-priori anatomical knowledge is enforced in a search algorithm selecting the best triplet. This triplet contains the final location of the OD.

Before running each independent weak detector, luminosity and contrast are normalized. To this purpose we have implemented the algorithm presented in [5]. This step converts an RGB coloured image into a normalized grey-scale image based only on the green channel. The red channel is discarded because it tends to be saturated and has less contrast than the green one, while the blue channel contains mainly noise.

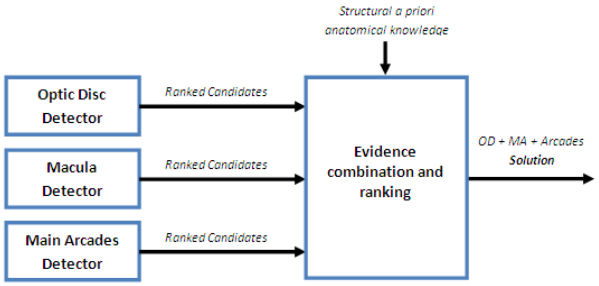

Fig. 1. Sketch of the methodology: 3 independent feature detectors are combined with anatomic knowledge to find the best solution

We shall now present the individual modules of the system, namely the weak detectors for arcades, OD and macula, triplet ranking, and search.

A. Arcades Detector

To locate the main arcades candidates, the normalized image is first smoothed using a bi-dimensional Gaussian filter. After that, 35 rows along and 20 columns are selected uniformly, forming a 55-line grid on the image. As vessels appear dark in the images we consider, 6 pixels with minimum intensity values found along each line are selected as initial candidate points to be part of the main arcades.

Next, each point is evaluated as a possible vessel point, and the width of the corresponding vessel, if any, is evaluated. Based on the idea that the intensity profile along a short vessel segment can be approximated by an inverted Gaussian, 5 different bi-dimensional masks (Gaussian cylinders) are created with different standard deviations to cater for various vessel widths (Figure 2). A sixth flat mask is added to detect points that not fitted satisfactorily by the Gaussian masks

(mainly low-contrast regions). To account for different orientations, each bi-dimensional mask is rotated in 11 different orientations (between 0° and 165° with a step of 15°).

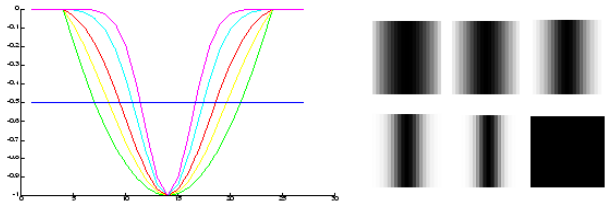

Fig. 2. The cross-section of the 6 different profiles (5 inverted Gaussians and the flat profile) and the 6 corresponding bi-dimensional patches

Each square region around the candidate point is normalized to a range between 0 and 1 and the Sum of Squared Distances (SSD) computed with each one of 56 masks (11 rotations times 5 profiles plus the flat one). If the region fits the flat profile best it is labeled as noise (non-vessel) and removed from the list of candidate points. An example of candidate vessel points can be seen in Figure 3 (left).

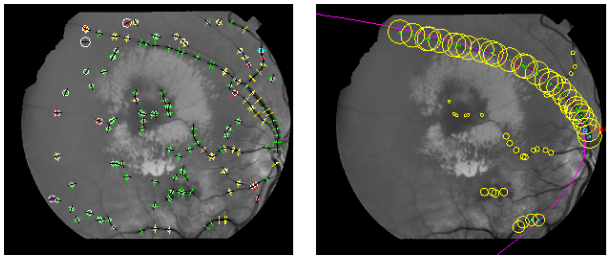

Fig. 3. The vessel candidates after removing noise which fits into the flat profile and the remaining points after grouping with the best parabola fitted with the General Hough Transform

To remove the false positive points remaining in the image, all the points are grouped using four criteria: the distance between points, the variance of the intensity cross-section, the angle between the orientation at the points. and the profiles of the fitting residuals. These are computed as follows:

$$path_{p,m} = \max\left(0.1 - \sigma, 0\right), \tag{1}$$

$$angle_{p,m} = \frac{\overrightarrow{O_p}\overrightarrow{O_m}}{\sqrt{\|p_{cx,cy} - m_{cx,cy}\|}}, \tag{2}$$

$$link_{p,m} = \frac{path_{p,m} \cdot \sqrt{angle_{p,m}}}{e_p \cdot e_m}, \tag{3}$$

where σ denotes the variance along a line between two candidate points p and m; $\overrightarrow{O_p}$, $\overrightarrow{O_m}$ are the unit vectors defined by the orientation of the points p and m; e_p, e_m the smallest (over all orientations and masks) fitting residuals at the two points and $p_{cx,cy}, m_{cx,cy}$ are the locations of p and m.

Only points within 40 pixels from each others are considered for efficiency. Then, the links are sorted in descending order and the top half (higher confidence) considered as correct links; the bottom half is discarded.

Next, the points are grouped. The widest point with the smallest error is considered the seed of a group, and expanded exploring the best two neighbours in each direction along the vessel. The grouping algorithm keeps exploring recursively both sides of the vessel, adding the best neighbour at each end based on their $link_{p,m}$ value and never changing the local direction of expansion more than 45°.

Finally, all the groups with three or less points are discarded, and the reliability r_g of each group g evaluated using the formula:

$$r_g = \sqrt{N}\frac{\frac{\sum_{n=1}^{N} c_n}{N}}{\frac{\sum_{n=1}^{N} e_n}{N}\frac{\sum_{n=1}^{N} w_n}{N}} \tag{4}$$

$$= \frac{1}{\sqrt{N}}\frac{\sum_{n=1}^{N} c_n}{\sum_{n=1}^{N} e_n \sum_{n=1}^{N} w_n}, \tag{5}$$

where c_n is the contrast, e_n the fitting errors and w_n the profile width rating of the n-th neighbour point.

Each point is assigned the rating of its group. All rated points are used as input to a Generalized Hough Transform (GHT) [1] finding the best-fit parabola over the set of points (Figure 3) (right).

The GHT accumulation matrix has 4 dimensions, 2 for the bi-dimensional space where the vertex of the parabola is located (using bins of 20 pixels in each dimension), 1 for the rotation of the parabola (with 14 degrees of freedom, distributed non-uniformly: 7 from -30° to 30° and another 7 between 150° and 210°, modelling images of left and right eye), and 13 bins for the amplitude of the parabola (between 9 and 81).

Finally, the 12 largest maxima in the accumulation matrix are returned as the 12 plausible candidates for the parabola. To rate the parabola reliability, the value in the corresponding bin of the accumulation matrix is used.

B. Optic Disc Detector

The OD appears normally as a bright circular zone with a radius around 60 pixels in the fundus images used and approximately centered vertically in the image. It is well-known that a computationally cheap and efficient way to find plausible OD candidates in images of healthy eyes is to smooth the image (removing noise and small bright spots) and detect the peaks in the intensity level map. Empirically we have observed that a healthy, well-imaged OD has a mean intensity level close to 0.15 higher than the mean of the whole image, so the rating formula becomes (truncated to 1):

$$\begin{cases} R_o^{OD} = \frac{Is_{x,y} - \bar{I}_s}{0.15} & \text{if } Is_{x,y} - \bar{I}_s < 0.15, \\ R_o^{OD} = 1 & \text{if } Is_{x,y} - \bar{I}_s \geq 0.15, \end{cases} \tag{6}$$

where $Is_{x,y}$ is the intensity value of the smoothed image at the coordinates x and y. The 0.15 threshold is likely to need adjusting for images acquired with different sensors,

although it has worked for fundus and SLO images in our experiments.

C. Macula Detector

The macula candidates are obtained in a similar way as the OD but with two main differences. First, to minimize false positives in the vessel structure, morphological closing is applied. Second, as the macula appears generally as a dark spot, the algorithm detects the valleys in the smoothed image instead of the peaks. Finally, as we consider that a healthy macula has a difference in intensity level not higher than 0.1 compared with the mean intensity level, the candidates are rated by:

$$\begin{cases} R_m^M = \frac{\bar{I}_s - Is_{x,y}}{0.10} & \text{if } \bar{I}_s - Is_{x,y} < 0.10, \\ R_m^M = 1 & \text{if } \bar{I}_s - Is_{x,y} \geq 0.10, \end{cases} \quad (7)$$

D. Triplet Ranking and Search

Although the number of OD and macula candidates cannot be controlled, experience indicates that the total amount of possible combinations between all plausible candidates will be a finite number not higher than a few hundreds. It is therefore possible to compute the rating of all the triplets by exhaustive search within a reasonable time.

The anatomical a-priori knowledge uses as reference the main arcades. For each computed parabola, all the OD and macula candidates are rated given their position in comparison with the parabola position and orientation. We use the expectation that the OD should be close to the vertex of the parabola (arcades convergence) and the macula should lie approximately along the axis of the parabola. Therefore a second rating score for all OD and macula candidates is computed given each arcade candidate:

$$R_{o,a}^{OD} = \frac{100}{\sqrt{dp_{o,a}^2 + 100^2}} \cdot \frac{150}{\sqrt{dv_{o,a}^2 + 150^2}} \cdot \frac{150}{\sqrt{dc_o^2 + 150^2}}, \quad (8)$$

$$R_{m,a}^{M} = \frac{100}{\sqrt{de_{m,a}^2 + 100^2}} \cdot \frac{150}{\sqrt{dc_m^2 + 150^2}}, \quad (9)$$

where $R_{o,a}^{OD}$ and $R_{o,a}^{M}$ are the rating for the OD candidate and macula respectively, $dp_{o,a}$ is the distance from the OD to the closest point of the parabola fitted over the arcades candidate, $dv_{o,a}$ is the distance from the OD candidate to the vertex of the parabola, $de_{m,a}$ is the distance between the position of the macula candidate and the expected position of the macula given the parabola (250 pixels away from the parabola vertex in the main axis direction). Finally, dc_o (resp. dc_m) is the distance between the OD (resp. MA) and the central height of the image, included as the vertically central part of the image is the most likely position for OD and macula.

Finally, the reliability of all the possible triplets is estimated with the formula:

$$rating_{o,m,a} = R_a^A (R_o^{OD} R_{o,a}^{OD})(\sqrt{R_m^M} R_{m,a}^M), \quad (10)$$

where R_a^A is the rating of the arcades. The combination with the highest confidence is selected as the final solution. As an example, Figure 4 shows the candidate set and the final solution.

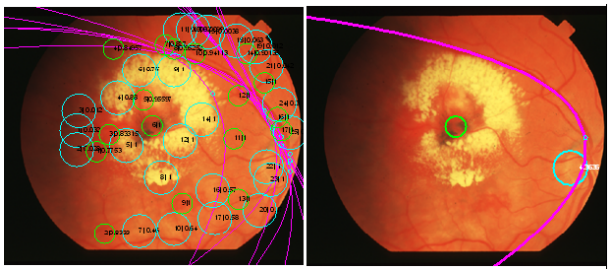

Fig. 4. Left: all candidates for OD, macula and arcades. Right: the final OD position candidate selected by our method.

III. Results

The proposed algorithm has been implemented in Matlab and initially tested using the 81 fundus images of the STARE project data set (35° field of view and 700×605 pixels of resolution) presented in [6]. In this data set 31 images are from healthy subjects whereas the other 50 contained pathological lesions of various types and severity. To validate the results we have manually identified the OD for ground truth and, as proposed in [6], the OD position was considered correctly detected if the estimates were inside the manually traced contour of the OD. The method presented in this paper is able to positively detect the OD location in 74 of the 81 images (91.4%) in the STARE data set: all the 31 healthy retinas and 43/50 (86%) of the diseased ones. The algorithm has also been tested with 20 images acquired by an OPTOS P200MA SLO (200 field of view, 3900×3072 pixels), containing various pathologies and distracting eyelid occlusions in a region surrounding the OD covering approximately the same region captured by STARE images. The algorithm detected the OD correctly in all the images.

The computing time of the entire process for a single image is around 30 seconds in the Matlab implementation, running on a pentium 4 at 3.0Ghz.

IV. Discussion

We have presented a novel algorithm to locate the optic disc in retinal images, leveraging context and multiple landmark candidates. The strength of this method is in the simultaneous use of context (OD, macula and main arcades) to locate a single one, the OD. The exploration of a number of plausible combinations of three landmarks gives the algorithm the capability to detect the OD in images with distracting pathologies, eye disease or eyelids. In 5 of the 7 images of the STARE data set where our method fails the OD is not present as completely occluded by a pathology lesion (im0005, im0010, im0020, im0026, im0044), while in the other 2 cases the main arcades are not correctly fitted due to bad image quality (im0004) or the main vessels are partially occluded with high tortuosity and distracting pathologies (im0001).

We also notice that, in clinical practice, images with completely obscured OD are either discarded as of poor quality, or referred to a clinician as containing serious lesions [3]; in either case, OD detection becomes superfluous. This seems to de-emphasize the applicative importance of automatic inference of invisible retinal landmarks. Finally, a qualitative comparison of correct detection percentages from methods reported recently in the literature suggests that our method performs well (Table I). It must be stressed that the figures in Table I refer to experiments conducted with a variety of conditions and image sets; their value is therefore only suggestive.

TABLE I

COMPARISON OF OUR METHOD AGAINST 4 DIFFERENT METHODS USING THE STARE DATA SET.

Algorithm	*Rate*
Constraint Satisfaction [10]	66.6%
Fuzzy Convergence [6]	88.9%
Combination of Weak Detectors	**91.4%**
Hough, Std and Bright Detectors Guided by Arcades [2]	93.8%
Geometric Model of Vessel Structure [4]	97.5%

In this approach only one kind of detector is used for each landmark, consequently if a landmark is no detected using this approach the algorithm has no alternative for it. The inclusion of different detectors focused on different properties of each landmark would be able to increase the robustness of the algorithm, while staying in the philosophy of the combination of several information of low quality to take a robust decision.

V. ACKNOWLEDGMENTS

Thanks go to Colin Buchanan for providing the OPTOS images and for technical discussions, and to the STARE projects for making their images publicly available.

REFERENCES

[1] D. H. Ballard. *Generalizing the Hough transform to detect arbitrary shapes*, pages 714–725. Morgan Kaufmann Publishers Inc., San Francisco, CA, USA, 1987.

[2] A D Fleming, K A Goatman, S. Philip, J A Olson, and P. Sharp. Automatic detection of retinal anatomy to assist diabetic retinopathy screening. *Physics in Medicine and Biology*, 52:331–345, 2007.

[3] Alan D. Fleming, Sam Philip, Keith A. Goatman, John A. Olson, , and Peter F. Sharp. Automated assessment of diabetic retinal image quality based on clarity and field definition. *Investigative Ophthalmology and Visual Science*, 47:1120–1125, 2006.

[4] Marco Foracchia, Enrico Grisan, and Alfredo Ruggeri. Detection of optic disc in retinal images by means of a geometrical model of vessel structure. *IEEE Trans. Med. Imaging*, 23(10):1189–1195, 2004.

[5] Marco Foracchia, Enrico Grisan, and Alfredo Ruggeri. Luminosity and contrast normalization in retinal images. *Medical Image Analysis*, 9(3):179–190, 2005.

[6] Adam Hoover and Michael H. Goldbaum. Locating the optical nerve in a retinal image using the fuzzy convergence of the blood vessels. *IEEE Trans. Med. Imaging*, 22(8):951–958, 2003.

[7] M Niemeijer, B van Ginneken, F van ter Haar, and M Abramoff. Automatic detection of optic disc, fovea and vascular arches in digital color photographs of the retina. In *Proc British Machine Vision Conf (BMVC'06)*, 2006.

[8] A Osareh, M Mirmehdi, B Thomas, and R Markham. Comparison of colour spaces for optic disc localisation in retinal images. In *Proc Int Conf on Pattern Recognition (ICPR)*, volume 1, pages 743–746, 2002.

[9] C. Sinthanayothin, J. Boyce, and C. T. Williamson. Automated localisation of the optic disc, fovea, and retinal blood vessels from digital colour fundus images. *British Journal of Ophthalmology*, 83:902–910, 1999.

[10] E Trucco and P J Kamat. Locating the optic disk in retinal images via plausible detection and constraint satisfaction. In *Proc. IEEE Int Conf on Image Processing (ICIP'04)*, pages 155–158, 2004.